Internal and External Atomic Steps in Graphite Exhibit Dramatically Different Physical and Chemical Properties

Hyunsoo Lee,[†,‡] Han-Bo-Ram Lee,[§] Sangku Kwon,[†,‡] Miquel Salmeron,*[,∥] and Jeong Young Park*[,†,‡]

[†]Center for Nanomaterials and Chemical Reactions, Institute for Basic Science (IBS), Daejeon 305-701, Republic of Korea, [‡]Graduate School of EEWS, Korea Advanced Institute of Science and Technology (KAIST), Daejeon 305-701, Republic of Korea, [§]Department of Materials Science and Engineering, Incheon National University, Incheon 406-772, Republic of Korea, and [∥]Materials Science Division, Lawrence Berkeley National Laboratory, Berkeley, California 94720, United States

ABSTRACT We report on the physical and chemical properties of atomic steps on the surface of highly oriented pyrolytic graphite (HOPG) investigated using atomic force microscopy. Two types of step edges are identified: internal (formed during crystal growth) and external (formed by mechanical cleavage of bulk HOPG). The external steps exhibit higher friction than the internal steps due to the broken bonds of the exposed edge C atoms, while carbon atoms in the internal steps are not exposed. The reactivity of the atomic steps is manifested in a variety of ways, including the preferential attachment of Pt nanoparticles deposited on HOPG when using atomic layer deposition and KOH clusters formed during drop casting from aqueous solutions. These phenomena imply that only external atomic steps can be used for selective electrodeposition for nanoscale electronic devices.

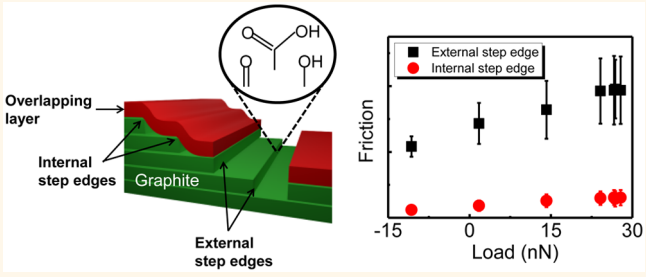

KEYWORDS: highly oriented pyrolytic graphite · surface reactivity · external and internal step edges · frictional force microscopy · atomic layer deposition

Graphite is composed of stacked planar graphene layers aligned in the Bernal *AB* sequence with weak van der Waals forces binding neighboring layers. The basal plane is a hexagonal honeycomb lattice of covalent sp^2 carbon bonds.[1] Most crystals exhibit many atomic steps that contain functional groups bound to edge carbon atoms with dangling and broken bonds,[2,3] which are responsible for the high chemical reactivity of step sites in comparison with the basal plane.

The frictional properties of the step edges on pristine graphene and graphite surfaces have been studied both experimentally and theoretically. Hölscher *et al.* reported the dependence of atomic-scale friction on the applied load at graphite step edges, depending on scan direction, using friction force microscopy (FFM).[4] The effect of the geometry of the FFM probe on atomic friction of the graphite step edges was studied also using molecular dynamics (MD) simulations.[5,6] Hunley *et al.* studied the frictional phenomena on two types of graphene step edges deposited on a silicon oxide layer. Two types of step edges were produced, covered and uncovered, due to overlapping graphene sheets deposited after the mechanical exfoliation process.[7] In UHV studies, T. Müller *et al.* reported that a step dislocation covered by a homogeneous graphite layer exhibits smaller friction than on a normal surface step with unsaturated sp^2 carbon bonds.[8] In addition, in air, adsorbed water molecules at the steps can influence energy dissipation processes, as shown by Egberts *et al.* on highly oriented pyrolytic graphite (HOPG) and consistent with MD simulations.[9] R. H. Savage *et al.* reported that the presence of water vapor is associated with increased wear on the graphite step edges and face,[10] and C. Sommerhalter *et al.* reported that the contact potential of HOPG is affected by the environmental conditions

* Address correspondence to mbsalmeron@lbl.gov, jeongypark@kaist.ac.kr.

Received for review November 26, 2014 and accepted March 27, 2015.

Published online March 27, 2015
10.1021/nn506755p

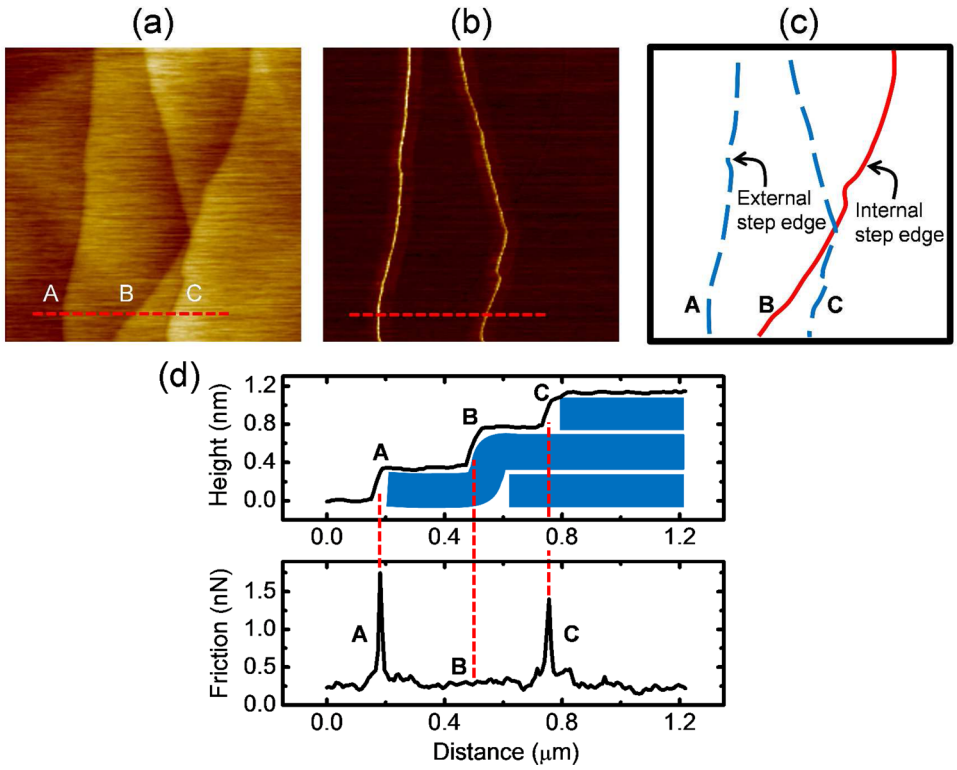

Figure 1. (a) 1.5 μm × 1.5 μm topography and (b) friction images of the HOPG (0001) surface measured in air after mechanical exfoliation with an applied load of 15 nN. (c) Schematic diagram showing two types of step edges on HOPG: internal (indicated by the red line) and external (indicated by the dashed blue lines). (d) Line profiles of the height and friction along the red dashed line in (a) and (b). The labels A and C represent external step edges, and label B denotes an internal step edge. All of the steps have a single-atom step height (0.34 nm). A Si tip was used for these measurements.

during sample cleavage and measurements.[11] These earlier studies focused on friction, wear, and chemical reactivity of external steps with exposed edges of the HOPG.

There are several studies associated with step edge decoration on HOPG.[12−14] In these studies, electrochemical methods were used to grow nanoscale particles and wires.[15−25] Xuan *et al*. reported different bonding energies between edge orientations (*e.g.*, armchair and zigzag) that induce the selective formation of Al_2O_3 nanowires using atomic layer deposition.[26]

In this paper, we report the observation of two types of atomic steps with different physical and chemical properties: external steps (generated by mechanical cleavage) and internal step edges (originating from graphite crystal growth). Friction imaging reveals a clear contrast in friction where a higher friction is found on the external steps, compared with internal steps. Contact potential difference (CPD) mapping also shows a different surface potential between external and internal steps. We show that the exposed external edges are highly reactive sites, as shown by the selective growth of Pt particles deposited using atomic layer deposition (ALD) and the precipitation of potassium hydroxide (KOH) clusters following drop casting. We also show that the higher reactivity of the external steps leads to higher atomic-scale wear.

RESULTS AND DISCUSSION

After mechanical cleavage of the pristine HOPG (0001) surface in air, we acquired topographical and friction images of the surface, as shown in Figure 1. The topographic image in Figure 1a, comprising step edges and terraces, was simultaneously acquired with the friction image shown in Figure 1b. The bright contrast in the friction image (Figure 1b) represents high friction. From the line profiles of height and friction, shown in Figure 1d, three steps (A, B, C) are visible. The height of all three steps is 0.34 nm, consistent with that of a single atomic step. Interestingly, only steps A and C show bright contrast in the friction images, while step B shows low friction, as shown in Figure 1d. On the basis of these measurements, we refer to atomic steps A and C as external steps and B as an internal step. In Figure 1c, the red line indicates an internal step edge and the blue lines indicate external step edges (Figure 1c). Similar FFM measurements on the HOPG surface, together with the feedback error signal (deflection), were performed on different areas of ZYB-grade HOPG (shown in Figures S1 and S2 in the Supporting Information, respectively) and also reveal two types of atomic steps. It should be noted that the ZYA-grade HOPG used in this study is of high quality (Grade SPI-1, SPI Supplies) with a low mosaic angle of 0.4 ± 0.1°, as shown in Figure S3 in the Supporting Information.

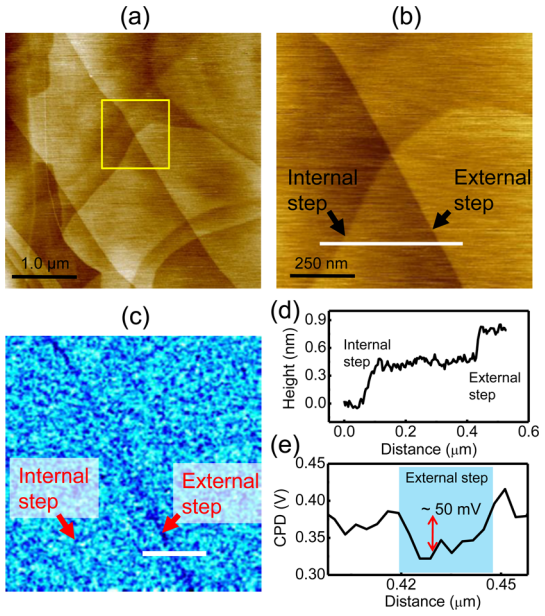

Figure 2. (a) Topography (4 μm $\times$ 4 μm) of the HOPG (0001) surface taken using noncontact-mode AFM. (b) Topography and (c) surface potential images (1 μm $\times$ 1 μm) of the yellow square in (a). The nearly straight line from the bottom right to top left is the external step, and the curved line is the internal step. The external step is easily distinguished from the internal step in the surface potential image. Line profiles showing the height (d) and surface potential (e), along the white solid line in (b) and (c), respectively. These two steps are monolayer-thick graphene. A PtIr-coated AFM tip was used for these measurements.

The dangling bonds on the steps, with the likely presence of adsorbates in air, should produce a change in CPD,[11] which is closely related to the local work function of the material. To obtain additional evidence about the internal and external steps, we carried out work function measurements of both types of step edges on the HOPG surface using Kelvin probe force microscopy (KPFM) in air. Figure 2 shows the results of KPFM in air (relative humidity of 46.8% and 23.9 °C) on the two types of step edges after mechanical cleavage for the fresh HOPG surface. Figure 2a shows the topography measured in noncontact-mode AFM. Figure 2b and c show the magnified topography and surface potential images of the yellow box in Figure 2a. The results in Figure 2b show a nearly straight line due to the external step running from the bottom-right corner to the top-left corner. This line is clearly distinguished from the other curved crosslines due to internal steps by its higher work function in Figure 2c. Both the internal and external steps followed the same friction behavior as that shown in Figure 1. Both steps are a single layer high in the cross line profile of Figure 2d. While the work function of the internal step is not distinguishable from that of the terrace, the work function of the external step was higher than that of the internal step or terraces by 50 mV, as shown in Figure 2e. We attribute this to unsaturated dangling bonds and oxygen terminations along the external

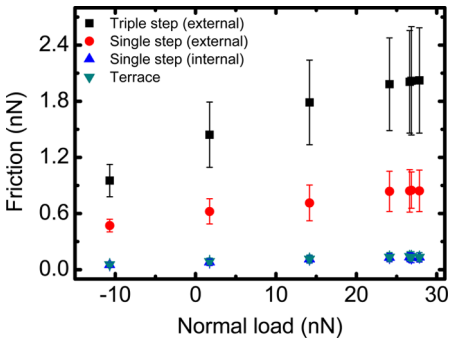

Figure 3. Plot of friction force *versus* applied normal force for three different types of steps: triple and single external step edges and single internal step edges. The friction on the step-free terrace is also shown as reference. A Si tip was used for these measurements.

step edge, which lead to enhancement of the dipole moment.[27] Contact potential mapping provides evidence that the external step edges are chemically and physically different from the internal steps of HOPG.

We investigated the load dependence of friction at both the external and internal step edges, as shown in Figure 3. The friction force is determined from the average values of the cantilever torsional deflection, after subtracting the trace (left to right) from the retrace (right to left) of the scan direction. Figure 3 shows the load dependence of the friction measured on external steps with single and triple atomic step heights, the internal step with a single atomic step height, and the terrace of the HOPG. The two external step edges (triple and single steps) show a mostly linear increase in friction with increasing load, while the friction only slightly increases at both the internal single step edge and the terrace. The Schwoebel–Ehrlich barrier, which is an energy barrier arising from reduced coordination of the edge atoms compared with that of the substrate atoms, is present only in the external step edge and is responsible for the observed increased friction.[28−30] We note that the adsorption of water at the external step edge has been proposed to also play a role in the enhancement of friction and wear at external steps.[9,10]

The different chemical reactivities of the two types of steps were further evidenced by depositing metal and KOH clusters on the HOPG surface. ALD was used to deposit Pt nanoparticles on the HOPG surface, where the exposed atoms of the external step edges provide nucleation sites for the Pt atoms. Lee *et al.* showed that Pt nanowires can be formed along the atomic steps of HOPG.[31] This is in line with the selective ALD of Pt metal at structural defect sites on CVD graphene, observed using transmission electron microscopy (TEM).[32]

Figure 4a,b show the topographical and friction images of the HOPG surface after 400 cycles of ALD for Pt deposition. As can be seen in Figure 4, both the topography and friction images show that one-dimensional Pt nanowires are formed only on the

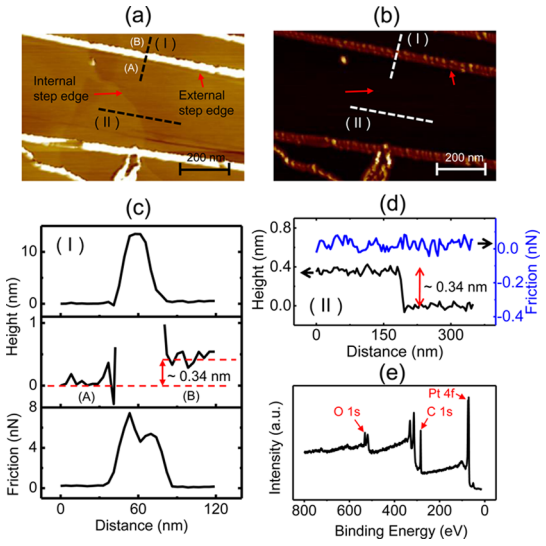

Figure 4. After 400 cycles of Pt ALD, (a) topography and (b) friction images (0.6 μm × 1.0 μm) were taken on the HOPG (0001) surface in air at an applied load of 12.5 nN. The linear bright regions in both images correspond to Pt nanowires formed by ALD at the external step edges. (c and d) Line profiles along (I) and (II), over single-layer steps with external and internal edges, respectively. It is clear that the Pt nanoparticles are selectively deposited on the external steps. A Si tip was used for these measurements. (e) X-ray photoelectron spectroscopy profiles of the HOPG sample showing peaks from the deposited Pt.

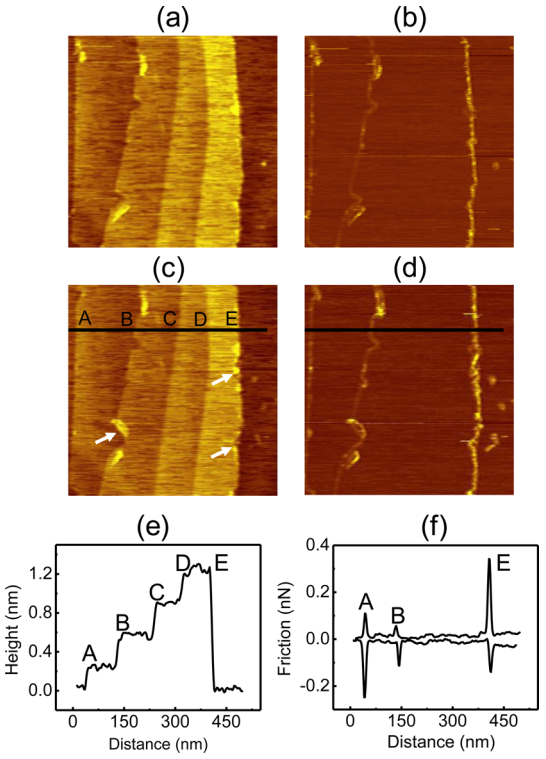

Figure 5. (a) Topography and (b) friction images (500 nm × 500 nm) of HOPG measured simultaneously under ultrahigh vacuum at an applied load of 20 nN. There are five atomic steps (A−E), including external (A, B, E) and internal (C, D) step edges. After scanning the area six times with an applied load of 6 nN, (c) topography and (d) friction images of the same area were taken. Only the external steps exhibit deformation, as noted by the white arrows, while the internal steps do not exhibit any change in morphology or friction. Line profiles of (e) height and (f) friction measured across the black solid line shown in (c) and (d). The heights of the step edges (A−D) in cross section are 0.34 nm (single step), and the atomic step (E) is four atomic layers. A TiN-coated tip was used for these measurements.

external step edges. Figure 4c,d show the line profiles of height and friction over single-layer steps with external (I) and internal (II) edges, respectively. The height and friction profiles show that the Pt nanowires formed at external step edges exhibit different growth rates (*i.e.*, the width and thickness of the Pt nanowire are about 40 and 14 nm, respectively) and have higher friction than that of the basal plane of the HOPG. In a previous paper, a difference between the lateral and vertical growth rates of Pt nanowires was also observed and explained by a change in the HOPG surface properties in the region where the ALD Pt forms.[31] However, as can be seen in Figure 4d, for monatomic internal steps the friction is undistinguishable from that of the basal plane. The unchanged step height (~0.34 nm) of the internal steps indicates no Pt deposition there, which is explained by the lack of reactive sites at these steps.[31] Figure 4e shows the results of X-ray photoelectron spectroscopy (XPS) showing Pt peaks due to the deposited nanoparticles, in addition to carbon and oxygen. The details of the XPS spectra for C 1s are described in Figure S4 in the Supporting Information.

We also investigated the formation of KOH nanodroplets that selectively formed on the external step edges, as shown in Figure S5 in the Supporting Information. Similar trends were reported by Hu *et al.*, who used atomic force microscopy (AFM) in noncontact electrostatic mode and observed that KOH nanodroplets formed on the HOPG step edges.[17]

The high reactivity of the external steps leads to facile atomic-scale wear. Figure 5 shows simultaneous topography and friction images (500 nm × 500 nm) of the HOPG under ultrahigh vacuum. Five steps are visible in the scanned area, which include external (A, B, E) and internal (C, D) step edges. After scanning the same area six times, topographical and friction images were taken, as shown in Figure 5c,d. Only the external steps exhibit wear, as noted by the white arrows in Figure 5c, while the internal steps do not exhibit any change in morphology. The high stress applied at the tip−sample proximity was high enough to cause wear on the external steps (due to higher reactivity). The stress can be easily calculated as the effective load/contact area. The contact area A can be obtained by using the Derjaguin−Muller−Toporov (DMT) model,[33−36] given by $A = \pi(R^{2/3}/K^{2/3})(L + L_c)^{2/3}$, where R is the curvature radius of the TiN-coated tip, K is the combined elastic modulus of graphite and the tip, L is the applied load, and L_c is the adhesion. Here, using $R = 50 \pm 10$ nm (as observed with scanning

electron microscopy), K = 530 GPa,[36,37] L = 6 nN, L_c = 21 nN, the contact area A is calculated as 5.86 nm^2. Thus, the applied stress is 27 nN/5.86 nm^2 = 4.61 GPa. This stress range at the tip−sample contact leads to wear on the external steps, while elastic contact is maintained on the internal steps and terraces.

Figure 5f shows different friction responses at the external steps between the trace and retrace scan directions associated with a Schwoebel−Ehrlich barrier.[4,30] We can rule out deformation of the tip because the friction images were stable and the friction signal on the terrace remained the same, as shown in Figure 5. When the HOPG surface is exposed to moist air, oxygen functional groups can adsorb on the chemically reactive external steps, which causes enhanced friction and wear. In our study, we carried out AFM measurements both in air and under UHV and confirmed the presence of two types of steps, as well as enhancement of friction at the external step. Therefore, we can rule out the effect of environment and humidity on the key results.

This study shows that atomic-scale wear takes place only on the external steps, which is associated with the high reactivity of the external steps. Our observation of different physical and chemical properties between the external and internal steps can be naturally applied to other layered materials.

CONCLUSIONS

In conclusion, we have shown that surface external step edges have a high friction contrast, a result that can be attributed to the existence of exposed dangling bonds, while no contrast is shown in the buried internal step edges of HOPG. A higher work function was observed on the external steps compared with other internal steps due to step dipoles and adsorbates. The selective formation of Pt nanowires and KOH nanoparticles using ALD and drop-casting methods, respectively, is due to the difference in chemical reactivity of both types of step edges. Atomic-scale wear takes place only on the external steps, which is also associated with the high reactivity of the external steps. This study indicates the presence of various overlapping layers that are easily distinguishable by friction measurements, suggesting potential applications in graphene-based nanoelectronic devices with selective electrochemical deposition.

EXPERIMENTAL SECTION

Materials and Methods. Pristine graphene sheets on graphite were fabricated from HOPG (0001) (Nano Technology Institute; the usual value of mosaic spread is 0.8 degree, the so-called ZYB grade) that is periodically stacked as 2D single-layer graphene along the *c*-axis with a relatively weak van der Waals interaction and composed of a hexagonal lattice of carbon with strong sp^2 bonding in the *a*, *b* plane.[1] Thus, graphene sheets were easily obtained using adhesive Scotch tape to peel off sheets from the bulk HOPG, which is a well-known mechanical exfoliation method.[38−40]

Pt ALD on a fresh HOPG (ZYB grade, K-TeK Nanotechnology) surface was performed using methylcyclopentadienyltrimethylplatinum ($MeCpPtMe_3$) for the Pt precursor and O_2 for the counter reactant. The vapor pressure was obtained by maintaining the Pt precursor container at 50 °C and the substrate at 300 °C. N_2 (30 sccm) was the carrier and purging gas in the ALD process.[31,41] The KOH droplets were prepared on a freshly cleaved HOPG surface using drop casting with a diluted KOH solution (concentration of 0.1 M in DI water). After 5 min, the diluted solution was visually removed by blowing air; the nanoscale KOH residues then remained on the HOPG surface.

Characterization. FFM and noncontact AFM measurements were carried out at ambient conditions (46−50% relative humidity and 23−24 °C) using an Agilent 5500 AFM. Similar experiments were carried out at UHV conditions using a RHK tech AFM/STM with a base pressure of 1.0 × 10^{-10} Torr.[42] We typically used Si (PPP-CONT, Nanosensors), Cr/Pt-coated (ElectriCont-G, Budget Sensors), and TiN-coated (CSG10, NT-MDT) AFM tips with the same typical force constant of 0.2 N/m for FFM; Pt/Ir-coated tips (PPP-EFM, Nanosensors) with a resonance frequency of 75 kHz were used for noncontact-mode AFM. The curvature radii of the Si and Cr/Pt-coated tips are <10 and <25 nm, and the resonant frequencies are 6−21 and 9−17 kHz, respectively. Since the measured friction force did not show time-dependent behavior during the experiments, we can consider that the range of stress during the measurements is in the elastic regime. The calibration constant of friction force was obtained by using a TGF11 silicon calibration grating sample (MikroMasch).[43,44]

KPFM measurements were also carried out at ambient conditions in a modified noncontact mode using an Agilent 5500 AFM. A PtIr-coated AFM tip (PPP-EFM-20, Nanosensor) was used (spring constant of 2.8 N/m (typical), resonance frequency of 75 kHz). Both the morphology and CPD were simultaneously measured by using two frequencies (ω_{mech} = 75 kHz, ω_{elec} = 10 kHz) in the single-path and interleave KPFM modes with amplitude modulation. The electrostatic interaction between the AFM probe and sample can be achieved by applying a tip bias V_{dc}. It can nullify the surface charge to make a zero value for the sinusoidal voltage signal in the total electrostatic force at the KPFM servo. The chemical composition of the Pt-deposited HOPG surface was characterized by XPS (Sigma Probe from Thermo VG Scientific) measurements under UHV (10^{-10} Torr) and using an Al Kα X-ray source (1486.3 eV).

Conflict of Interest: The authors declare no competing financial interest.

Acknowledgment. This work was supported by IBS-R004-G4. M.S. was supported by the "Chemical and Mechanical Properties of Surfaces, Interfaces and Nanostructures" program, Office of Basic Energy Sciences, Division of Materials Sciences and Engineering, U.S. Department of Energy, under Contract No. DE-AC02-05CH11231.

Supporting Information Available: Friction force microscopy images of the surface of multistacked layers on HOPG (Figure S1) and ZYB-grade (Figure S2) and ZYA-grade (Figure S3) HOPG. X-ray photoelectron spectroscopy analysis of the Pt-deposited HOPG surface (Figure S4). Noncontact scan images of KOH clusters on the external steps (Figure S5). This material is available free of charge *via* the Internet at http://pubs.acs.org.

REFERENCES AND NOTES

1. Kelly, B. T. *Physics of Graphite*; Applied Science: London, 1981; p 477.
2. Xiao, Y. K.; Yu, G.; Yuan, J.; Wang, J. Y.; Chen, Z. Z. Fabrication of Pd-Ni Alloy Nanowire Arrays on HOPG Surface by Electrodeposition. *Electrochim. Acta* **2006**, *51*, 4218–4227.

3. Ji, X. B.; Banks, C. E.; Xi, W.; Wilkins, S. J.; Compton, R. G. Edge Plane Sites on Highly Ordered Pyrolytic Graphite as Templates for Making Palladium Nanowires *via* Electrochemical Decoration. *J. Phys. Chem. B* **2006**, *110*, 22306–22309.
4. Holscher, H.; Ebeling, D.; Schwarz, U. D. Friction at Atomic-Scale Surface Steps: Experiment and Theory. *Phys. Rev. Lett.* **2008**, *101*, 246105.
5. Dong, Y. L.; Liu, X. Z.; Egberts, P.; Ye, Z. J.; Carpick, R. W.; Martini, A. Correlation between Probe Shape and Atomic Friction Peaks at Graphite Step Edges. *Tribol. Lett.* **2013**, *50*, 49–57.
6. Ye, Z. J.; Otero-de-la-Roza, A.; Johnson, E. R.; Martini, A. Effect of Tip Shape on Atomic-Friction at Graphite Step Edges. *Appl. Phys. Lett.* **2013**, *103*, 081601.
7. Hunley, D. P.; Flynn, T. J.; Dodson, T.; Sundararajan, A.; Boland, M. J.; Strachan, D. R. Friction, Adhesion, and Elasticity of Graphene Edges. *Phys. Rev. B* **2013**, *87*, 035417.
8. Müller, T.; Lohrmann, M.; Kässer, T.; Marti, O.; Mlynek, J.; Krausch, G. Frictional Force between a Sharp Asperity and a Surface Step. *Phys. Rev. Lett.* **1997**, *79*, 5066–5069.
9. Egberts, P.; Ye, Z.; Liu, X. Z.; Dong, Y.; Martini, A.; Carpick, R. W. Environmental Dependence of Atomic-Scale Friction at Graphite Surface Steps. *Phys. Rev. B* **2013**, *88*, 035409.
10. Savage, R. H. Graphite Lubrication. *J. Appl. Phys.* **1948**, *19*, 1–10.
11. Sommerhalter, C.; Matthes, T. W.; Glatzel, T.; Jäger-Waldau, A.; Lux-Steiner, M. C. High-Sensitivity Quantitative Kelvin Probe Microscopy by Noncontact Ultra-High-Vacuum Atomic Force Microscopy. *Appl. Phys. Lett.* **1999**, *75*, 286–288.
12. Menke, E. J.; Li, Q.; Penner, R. M. Bismuth Telluride (Bi_2Te_3) Nanowires Synthesized by Cyclic Electrodeposition/Stripping Coupled with Step Edge Decoration. *Nano Lett.* **2004**, *4*, 2009–2014.
13. Walter, E. C.; Zach, M. P.; Favier, F.; Murray, B. J.; Inazu, K.; Hemminger, J. C.; Penner, R. M. Metal Nanowire Arrays by Electrodeposition. *ChemPhysChem* **2003**, *4*, 131–138.
14. Wang, X.; Tabakman, S. M.; Dai, H. Atomic Layer Deposition of Metal Oxides on Pristine and Functionalized Graphene. *J. Am. Chem. Soc.* **2008**, *130*, 8152–8153.
15. Boxley, C. J.; White, H. S.; Lister, T. E.; Pinhero, P. J. Electrochemical Deposition and Reoxidation of Au at Highly Oriented Pyrolytic Graphite. Stabilization of Au Nanoparticles on the Upper Plane of Step Edges. *J. Phys. Chem. B* **2003**, *107*, 451–458.
16. Losic, D.; Martini, L. L.; Aguilar, M. I.; Small, D. H. Beta-Amyloid Fibril Formation is Promoted by Step Edges of Highly Oriented Pyrolytic Graphite. *Biopolymers* **2006**, *84*, 519–526.
17. Hu, J.; Carpick, R. W.; Salmeron, M.; Xiao, X. D. Imaging and Manipulation of Nanometer-Size Liquid Droplets by Scanning Polarization Force Microscopy. *J. Vac. Sci. Technol., B* **1996**, *14*, 1341–1343.
18. Li, Q. G.; Olson, J. B.; Penner, R. M. Nanocrystalline Alpha-MnO_2 Nanowires by Electrochemical Step-Edge Decoration. *Chem. Mater.* **2004**, *16*, 3402–3405.
19. Zach, M. P.; Newberg, J. T.; Sierra, L.; Hemminger, J. C.; Penner, R. M. Chemical Vapor Deposition of Silica Micro- and Nanoribbons Using Step-Edge Localized Water. *J. Phys. Chem. B* **2003**, *107*, 5393–5397.
20. Zach, M. P.; Inazu, K.; Ng, K. H.; Hemminger, J. C.; Penner, R. M. Synthesis of Molybdenum Nanowires with Millimeter-Scale Lengths Using Electrochemical Step Edge Decoration. *Chem. Mater.* **2002**, *14*, 3206–3216.
21. Taing, J.; Cheng, M. H.; Hemminger, J. C. Photodeposition of Ag or Pt onto TiO_2 Nanoparticles Decorated on Step Edges of HOPG. *ACS Nano* **2011**, *5*, 6325–6333.
22. Diculescu, V. C.; Chiorcea-Paquim, A. M.; Corduneanu, O.; Oliveira-Brett, A. M. Palladium Nanoparticles and Nanowires Deposited Electrochemically: AFM and Electrochemical Characterization. *J. Solid State Electrochem.* **2007**, *11*, 887–898.
23. Xiao, Y.; Weng, B.; Yu, G.; Wang, J.; Hu, B.; Chen, Z. Electrodeposition of Pd−Ag Alloy Nanowires on Highly Oriented Pyrolytic Graphite. *J. Appl. Electrochem.* **2006**, *36*, 807–812.
24. Tang, L.; Yu, G.; Ouyang, Y.; Si, W.; Weng, B. Single Pulse Deposition of Pd−Ag Alloy Nanowires on Highly Oriented Pyrolytic Graphite: A Mechanistic Assessment. *Electrochim. Acta* **2008**, *53*, 3305–3312.
25. Scott, S. A.; Kral, M. V.; Brown, S. A. Growth of Oriented Bi Nanorods at Graphite Step-Edges. *Phys. Rev. B* **2005**, *72*, 205423.
26. Xuan, Y.; Wu, Y. Q.; Shen, T.; Qi, M.; Capano, M. A.; Cooper, J. A.; Ye, P. D. Atomic-Layer-Deposited Nanostructures for Graphene-Based Nanoelectronics. *Appl. Phys. Lett.* **2008**, *92*, 013101.
27. Ramprasad, R.; Allmen, P. v.; Fonseca, L. R. C. Contributions to the Work Function: A Density-Functional Study of Adsorbates at Graphene Ribbon Edges. *Phys. Rev. B* **1999**, *60*, 6023–6027.
28. Schwoebel, R. L.; Shipsey, E. J. Step Motion on Crystal Surfaces. *J. Appl. Phys.* **1966**, *37*, 3682–3686.
29. Ehrlich, G. Atomic Displacements in One- and Two-Dimensional Diffusion. *J. Chem. Phys.* **1966**, *44*, 1050–1055.
30. Steiner, P.; Gnecco, E.; Krok, F.; Budzioch, J.; Walczak, L.; Konior, J.; Szymonski, M.; Meyer, E. Atomic-Scale Friction on Stepped Surfaces of Ionic Crystals. *Phys. Rev. Lett.* **2011**, *106*, 186104.
31. Lee, H. B. R.; Baeck, S. H.; Jaramillo, T. F.; Bent, S. F. Growth of Pt Nanowires by Atomic Layer Deposition on Highly Ordered Pyrolytic Graphite. *Nano Lett.* **2013**, *13*, 457–463.
32. Kim, K.; Johnson, R. W.; Tanskanen, J. T.; Liu, N.; Kim, M.-G.; Pang, C.; Ahn, C.; Bent, S. F.; Bao, Z. Selective Metal Deposition at Graphene Line Defects by Atomic Layer Deposition. *Nat. Commun.* **2014**, *5*, 4781.
33. Derjaguin, B. V.; Muller, V. M.; Toporov, Y. P. Effect of Contact Deformations on the Adhesion of Particles. *J. Colloid Interface Sci.* **1975**, *53*, 314–326.
34. Enachescu, M.; van den Oetelaar, R. J. A.; Carpick, R. W.; Ogletree, D. F.; Flipse, C. F. J.; Salmeron, M. Atomic Force Microscopy Study of an Ideally Hard Contact: The Diamond(111)/Tungsten Carbide Interface. *Phys. Rev. Lett.* **1998**, *81*, 1877–1880.
35. Park, J. Y.; Salmeron, M. Fundamental Aspects of Energy Dissipation in Friction. *Chem. Rev.* **2014**, *114*, 677–711.
36. Park, J. Y.; Ogletree, D. F.; Salmeron, M.; Ribeiro, R. A.; Canfield, P. C.; Jenks, C. J.; Thiel, P. A. Tribological Properties of Quasicrystals: Effect of Aperiodic versus Periodic Surface Order. *Phys. Rev. B* **2006**, *74*, 024203.
37. Blakslee, O. L.; Proctor, D. G.; Seldin, E. J.; Spence, G. B.; Weng, T. Elastic Constants of Compression-Annealed Pyrolytic Graphite. *J. Appl. Phys.* **1970**, *41*, 3373–3382.
38. Allen, M. J.; Tung, V. C.; Kaner, R. B. Honeycomb Carbon: A Review of Graphene. *Chem. Rev.* **2009**, *110*, 132–145.
39. Novoselov, K. S.; Fal, V.; Colombo, L.; Gellert, P.; Schwab, M.; Kim, K. A Roadmap for Graphene. *Nature* **2012**, *490*, 192–200.
40. Rao, C. N. R.; Sood, A. K.; Subrahmanyam, K. S.; Govindaraj, A. Graphene: The New Two-Dimensional Nanomaterial. *Angew. Chem., Int. Ed.* **2009**, *48*, 7752–7777.
41. Lee, H. B. R.; Bent, S. F. Microstructure-Dependent Nucleation in Atomic Layer Deposition of Pt on TiO_2. *Chem. Mater.* **2012**, *24*, 279–286.
42. Kwon, S.; Choi, S.; Chung, H. J.; Yang, H.; Seo, S.; Jhi, S.-H.; Park, J. Y. Probing Nanoscale Conductance of Monolayer Graphene under Pressure. *Appl. Phys. Lett.* **2011**, *99*, 013110.
43. Ogletree, D. F.; Carpick, R. W.; Salmeron, M. Calibration of Frictional Forces in Atomic Force Microscopy. *Rev. Sci. Instrum.* **1996**, *67*, 3298–3306.
44. Varenberg, M.; Etsion, I.; Halperin, G. An Improved Wedge Calibration Mehod for Lateral Force in Atomic Force Microscopy. *Rev. Sci. Instrum.* **2003**, *74*, 3362–3367.